Relating Environmental Effects and Structures, IR, and NMR Properties of Hydrogen-Bonded Complexes: ClH:Pyridine

Karena Chapman, Deborah Crittenden, Joseph Bevitt, and Meredith J. T. Jordan

School of Chemistry, University of Sydney, Sydney, NSW 2006, Australia

Janet E. Del Bene*

Department of Chemistry, Youngstown State University, Youngstown, Ohio 44555, and Quantum Theory Project, University of Florida, Gainesville, Florida 32611

Received: December 7, 2000; In Final Form: March 12, 2001

MP2/aug′-cc-pVDZ potential surfaces for the hydrogen-bonded complex ClH:pyridine have been generated without and with external electric fields. The zero-field, gas-phase structure of this complex is stabilized by a traditional Cl−H···N hydrogen bond. As the field strength increases, the equilibrium structure changes to that of a proton-shared hydrogen-bonded complex, which is close to quasi-symmetric at a field of 0.0040 au, and then an ion-pair complex at higher fields. Anharmonic dimer- and proton-stretching frequencies have been computed from each surface, and compared to experimental frequencies in Ar and N_2 matrices. The computed results suggest that the hydrogen bond in ClH:pyridine is on the traditional side of quasi-symmetric in an Ar matrix, and on the ion-pair side in an N_2 matrix. EOM-CCSD and MP2 calculations have been performed on the equilibrium structure at each field strength to obtain the $^{35}Cl-^{15}N$ spin−spin coupling constant across the hydrogen bond, and the chemical shift of the hydrogen-bonded proton, respectively. As a function of field strength, the Cl−N distance, the proton-stretching frequency, and the Cl−N coupling constant exhibit extrema for the quasi-symmetric complex found at a field of 0.0040 au. These IR and NMR properties are fingerprints of hydrogen bond type from which the intermolecular distance in a complex may be determined. The chemical shift of the hydrogen-bonded proton is also a maximum at a field of 0.0040 au, but it does not decrease dramatically at higher fields, and may not be as useful for structure determination. Deuteration of HCl lowers the proton-stretching frequency, as expected. The two-dimensional anharmonic proton-stretching frequencies for ClD:pyridine, as a function of field strength, show the same pattern as the ClH:pyridine frequencies.

Introduction

In a previous paper, we examined the structures and anharmonic dimer- and proton-stretching frequencies in complexes with HCl and HBr as proton donors, and NH_3 and $N(CH_3)_3$ as proton acceptors.[1] The equilibrium structures of the complexes with NH_3 are stabilized by traditional hydrogen bonds, in which the HCl and HBr molecules remain essentially intact. In contrast, the equilibrium structure of $ClH:N(CH_3)_3$ has a proton-shared hydrogen bond, with relatively long Cl−H and N−H distances, but with a short Cl−N distance. The equilibrium structure of $BrH:N(CH_3)_3$ approaches that of an ion-pair complex after proton transfer from Br to N. We employed isotropic external electric fields, by analogy with Onsager's model for dipolar fluids,[2] as a simple model to emulate matrix effects. An external field preferentially stabilizes more polar structures, so hydrogen bond type changes from traditional, to proton-shared, to ion-pair as the field strength increases. Changes in proton-stretching frequencies were found to parallel changes in hydrogen bond type. For example, the complex $ClH:NH_3$ has a traditional hydrogen bond at zero field, and the proton-stretching vibration is aptly described as a perturbed Cl−H stretch. The frequency of this vibration initially decreases as a field is applied, exhibits a minimum when the hydrogen bond becomes a quasi-symmetric proton-shared hydrogen bond, and then subsequently increases as the proton-stretching vibration becomes a perturbed N−H stretch in a hydrogen-bonded ion-pair. The results of this study provided insight into field effects on proton-stretching frequencies, and the basis for interpreting the experimental low-temperature vibrational spectra observed for these complexes and their deuterated analogues[3] in Ar and N_2 matrices. Other investigators have also examined the effects of electric fields or the presence of ions on proton-transfer and other properties of hydrogen-bonded complexes.[4−7]

In a subsequent study of the $ClH:NH_3$ complex, we demonstrated that the intermolecular distance, the proton-stretching frequency, and the NMR properties of proton chemical shift of the hydrogen-bonded proton and Cl−N coupling constant across the hydrogen bond behave similarly with respect to an applied external field.[8] That is, plots of these properties as a function of external field exhibit extrema at the same field strength. Thus, these IR and NMR spectroscopic properties are fingerprints of hydrogen bond type and can be used to obtain structural information about hydrogen-bonded complexes. We note that, since ^{35}Cl and ^{37}Cl have nonzero quadrupole moments, Cl−N coupling constants have not been experimentally observed. However, the structures and vibrational spectra of complexes with Cl−N hydrogen bonds have been relatively well studied both experimentally and theoretically.[1,3,8−14] These complexes are appealing theoretical models and we expect the trends observed among structures, IR proton-stretching frequencies,

10.1021/jp004409m CCC: $20.00
Published on Web 05/15/2001

and NMR properties to be valid for a wide range of hydrogen-bonded complexes. To further investigate the generality of these relationships, we have extended our studies to the ClH:pyridine complex.

Methods

The structure of ClH:pyridine has been optimized at zero field under the constraint of C_{2v} symmetry using second-order many-body Møller−Plesset perturbation theory [MBPT(2) = MP2)][15−18] with the Dunning correlation-consistent polarized valence double-split basis set augmented with diffuse s, p, and d functions on nonhydrogen atoms (aug′-cc-pVDZ).[19−21] The monomers HCl and pyridine were optimized at the same level of theory. Harmonic vibrational frequencies were computed to confirm equilibrium structures, to simulate harmonic vibrational spectra, and to obtain zero-point vibrational energy contributions to the binding enthalpy at 10 K (ΔH_h[10]), the temperature at which matrix isolation measurements are made. The subscript "h" is used to denote that the zero-point energy correction has been evaluated exclusively from harmonic frequencies, as is usually done. However, since the potential surface describing the proton-stretching vibration can be very anharmonic, using the harmonic zero-point energy for this mode may lead to a relatively large error.[1] Anharmonic zero-point energy corrections have been estimated by replacing the harmonic zero-point energies of the dimer and proton stretches with the anharmonic zero-point energy obtained from the two-dimensional surface (as outlined below) and also using the anharmonic zero-point energy for the HCl monomer.[9] The resulting binding enthalpy at 10 K is denoted ΔH_a.[10]

Optimization, frequency, and single-point calculations to generate potential surfaces without and with external electric fields were accomplished by freezing the s and p electrons below the valence shells in the Hartree−Fock molecular orbitals. This level of theory produces reliable structures and vibrational frequency shifts for the proton-stretching band of a complex relative to the monomer, if the anharmonicity correction in the complex is not large, and a reasonable estimate of binding energies.[22−25] However, it should be noted that the computed binding energy is overestimated since neither the wave function model nor the basis set is converged. The objective of the present study is not to provide quantitatively accurate binding energies, but to show how potential surfaces obtained at an appropriate level of theory change with external field strength, and how the variation in structural and IR and NMR spectroscopic properties parallel this change.

Two-dimensional potential energy surfaces were generated by freezing the pyridine coordinates in a manner similar to earlier work,[1] and then varying the N−H and Cl−H distances. Results at nonzero fields were obtained by applying external fields of varying strengths along the hydrogen bonding Cl−H−N axis. The ab initio surfaces were spanned by varying the intermolecular Cl−N distance from 2.60 to 3.30 Å in steps of 0.05 Å. At each Cl−N distance, the Cl−H distance was initially set to 1.10 Å and then incremented in steps of 0.05 Å until the N−H distance was 0.90 Å. The ab initio data cover the most chemically relevant areas of the potential surfaces including those regions associated with traditional, proton-shared, and ion-pair hydrogen bonds, and extend sufficiently far to describe the walls of these surfaces.

Global potential energy surfaces were constructed from the ab initio data, using the procedure outlined in ref 1, and "augmented" rectangular grids of data points were generated. Bicubic spline interpolation was used to describe the potential energy surface within these grids and polynomial extrapolation was used outside the grids. At short bond lengths a quadratic extrapolation was used and at long bond lengths the extrapolation was linear. The procedure used is robust, and has been effectively automated.

The resulting two-dimensional potential energy surfaces describe a pseudo-triatomic system, A−H−B, where A represents the pyridine and B the chlorine. The bond lengths R_1 and R_2 are the distance from H to the center-of-mass of pyridine, and the Cl−H distance, respectively. Where appropriate, R_1 has been subsequently transformed back to the N−H distance. Minimum energy configurations and harmonic frequencies were obtained on the pseudo-triatomic surfaces using normal-mode analyses.

Two-dimensional vibrational eigenfunctions and eigenvalues were calculated as previously,[1] using a model Hamiltonian for the collinear A−H−B system in the R_1 and R_2 coordinates described above. Eigenfunctions were calculated variationally using the discrete variable representation (DVR)[26] of a two-dimensional basis set constructed as a direct product of one-dimensional tridiagonal Morse functions,[27] each optimized to an appropriate one-dimensional Schrödinger equation. The results quoted below used 120:60 primitive:contracted basis functions in each coordinate, and the vibrational eigenvalues are converged to better than 0.1 cm^{-1}.

One-dimensional eigenvectors and eigenvalues were also calculated along either the proton or the dimer stretching normal mode displacement vector, as obtained from a normal-mode analysis of the two-dimensional pseudo-triatomic potential surface. Tridiagonal Morse basis functions were again used to expand the vibrational wave functions, and the eigenvalues are converged to better than 0.1 cm^{-1}.

The sensitivity of the calculated vibrational eigenvalues to the procedures used to extrapolate to a global potential energy surface was also examined. Augmented potential grids were created using linear or quadratic extrapolation, and global surfaces were formed using all combinations of zeroth-, first-, and second-order polynomial extrapolation. Uncertainties in the calculated vibrational eigenvalues were estimated as the maximum deviation observed as the potential energy surface was varied. These values were approximately 1 cm^{-1} for the anharmonic two-dimensional dimer-stretching frequency and 3 cm^{-1} for the anharmonic two-dimensional proton-stretching frequency. The harmonic and one-dimensional anharmonic results differed by less than 1 cm^{-1} as the surfaces were varied.

Equation-of-motion coupled cluster singles and doubles calculations (EOM-CCSD)[28−31] using the configuration-interaction (CI-like) approximation were carried out to obtain two-bond $^{35}Cl-^{15}N$ spin−spin coupling constants ($^{2h}J_{Cl-N}$) across the hydrogen bond for the equilibrium ClH:pyridine structure at each field strength. The symbol ^{2h}J is used to indicate two-bond coupling across a hydrogen bond. There are four terms that contribute to the total spin−spin coupling constant, namely, the paramagnetic spin−orbit, diamagnetic spin−orbit, Fermi-contact, and spin dipole. For N−H−N, N−H−O, O−H−O, and Cl−H−N hydrogen bonds, the spin−spin coupling constant $^{2h}J_{X-Y}$ is dominated by the Fermi-contact term, which is more than an order of magnitude greater than any other term.[8,32] In ref 8, for example, the magnitude of the Fermi-contact term was found to be no more than 4% larger than that of the total $^{2h}J_{Cl-N}$ coupling constant for equilibrium structures of $ClH:NH_3$ at various field strengths. Therefore, $^{2h}J_{Cl-N}$ for ClH:pyridine has been estimated solely from the Fermi-contact term. The EOM-CCSD calculations employed the Ahlrichs[33] qzp basis set

TABLE 1: Dipole Moment, Cavity Radius, and Onsager Reaction Field at the Equilibrium Geometry of ClH:NH_3, ClH:$N(CH_3)_3$, and ClH:Pyridine at $\epsilon = 1.6$ and 2.0

			field (au)	
species	dipole (D)	cavity radius (au)	$\epsilon = 1.6$	$\epsilon = 2.0$
ClH:NH_3[a]	4.71	6.17	0.0023	0.0032
ClH:$N(CH_3)_3$	8.49	7.77	0.0020	0.0028
ClH:pyridine	6.56	8.14	0.0014	0.0019

[a] There are typographical errors in these quantities in Table 6 of ref 1.

on Cl, N, and C atoms, qz2p on the hydrogen-bonded proton, and the Dunning cc-pVDZ basis set[19−21] on the pyridine hydrogens. This level of theory has been used in previous studies to obtain coupling constants in a variety of hydrogen-bonded systems and has been shown to produce quantitatively accurate coupling constants (without rescaling) when compared to experimentally measured values, and to have predictive value.[8,32,34−36] Proton chemical shifts were computed at MBPT-(2) with the same basis set using the gauge-invariant atomic orbital (GIAO) method.[37]

In this work we have employed isotropic external electric fields, by analogy with Onsager's model for dipolar fluids,[2] as a simple model to emulate matrix effects. Appropriate field strengths for Ar and N_2 matrices may be estimated (as in ref 1) by approximating the Onsager reaction field, **R**, as

$$\mathbf{R} = [2(\epsilon - 1)]/(2\epsilon + 1)\mu/a^3 \qquad (1)$$

where ϵ is the relative permittivity of the dielectric medium, μ is the permanent dipole moment of the complex, and a is its cavity radius. The permanent dipole moment μ has been calculated at the MP2/aug′-cc-pVDZ level of theory. The cavity radius a may be calculated by determining the volume contained within the 0.001 au electron density surface around the complex, equating this volume to the volume of a sphere of radius r and setting $a = r + 0.5$ Å.[38] For illustrative purposes the Onsager reaction field has been calculated at $\epsilon = 1.6$, representing solid Ar at 10 K,[39] and $\epsilon = 2.0$ as an indication of the likely effects of an N_2 matrix.[1] Results for ClH:pyridine are compared with those for ClH:NH_3 and ClH:$N(CH_3)_3$ in Table 1.

Gaussian 98[38] was used to optimize the zero-field geometries of HCl, pyridine, and the ClH:pyridine complex, to compute harmonic vibrational frequencies, and to generate the ab initio data points for the potential energy surfaces without and with electric fields. Spin−spin coupling constants and proton chemical shifts were computed using the ACES II program.[40] These calculations were carried out on the SGI−Origin and the Cray SV1 computers at the Ohio Supercomputer Center, and the computing facilities at the University of Sydney.

Results and Discussion

Structural and IR Results without an External Field. The zero-field structure of ClH:pyridine has computed Cl−N and Cl−H distances (R_e) of 2.976 and 1.366 Å, respectively, as reported in Table 2. The computed Cl−H distance is elongated by 0.078 Å relative to the HCl monomer. Legon has concluded from gas-phase microwave structural data that in the ClH:pyridine complex the proton is not transferred from Cl to N.[12] Our computed structure is in agreement with this conclusion. However, although the equilibrium structure of this complex is stabilized by a traditional Cl−H···N hydrogen bond, the degree of proton transfer from Cl to N is greater than in the ClH:NH_3 complex, which has Cl−N and Cl−H distances (R_e) of 3.080 and 1.341 Å, respectively. The MP2/aug′-cc-pVDZ binding energy (ΔE_e) of ClH:pyridine is −11.0 kcal/mol, which is greater than the ClH:NH_3 binding energy of −9.5 kcal/mol. The zero-point vibrational energy contribution obtained from the harmonic frequencies is + 1.5 kcal/mol, leading to a binding enthalpy of ClH:pyridine of −9.5 kcal/mol at 10 K (ΔH_h[10]). When anharmonic zero-point vibrational energies for the proton- and dimer-stretching modes are used instead, the zero-point vibrational energy correction is + 1.1 kcal/mol, leading to a binding enthalpy (ΔH_a[10]) of −9.9 kcal/mol. The error introduced by using the harmonic zero-point energies is 0.4 kcal/mol, which is greater than that found for ClH:NH_3, but less than that for ClH:$N(CH_3)_3$. The latter complex has a gas-phase equilibrium structure stabilized by a proton-shared hydrogen bond.[1]

TABLE 2: Equilibrium Cl−N and Cl−H Distances [R_e(Cl−N), R_e(Cl−H), Å] and Expectation Values of the Cl−N and Cl−H Distances [R_0(Cl−N), R_0(Cl−H), Å] in the Ground Vibrational State for ClH:Pyridine as a Function of Field Strength (au)

field	R_e(Cl−N)	R_e(Cl−H)	R_0(Cl−N)	R_0(Cl−H)
0.0000	2.976	1.366	2.914	1.444
0.0010	2.941	1.383	2.889	1.473
0.0020	2.893	1.416	2.873	1.505
0.0040	2.820	1.605	2.860	1.570
0.0055	2.842	1.679	2.863	1.618
0.0100	2.934	1.834	2.922	1.769

The harmonic and anharmonic dimer- and proton-stretching frequencies are reported in Table 3. The harmonic dimer-stretching frequency obtained from the full 33-dimensional surface is 128 cm^{-1}. This value is slightly lower than the harmonic and the one-dimensional anharmonic frequencies obtained from the two-dimensional zero-field surface, which have values of 140 and 144 cm^{-1}, respectively. The two-dimensional anharmonic frequency is 185 cm^{-1}. The differences between the harmonic and anharmonic frequencies for the proton-stretching mode are greater. The harmonic frequencies obtained from the full-dimensional calculation and from the two-dimensional surface are similar at 1964 and 1954 cm^{-1}, respectively. These frequencies are notably greater than the anharmonic one- and two-dimensional frequencies of 1365 and 1289 cm^{-1}, respectively. The difference between the one- and two-dimensional anharmonic frequencies is significantly less than it is for ClH:NH_3, suggesting that the degree of coupling between the dimer and the proton stretching vibrations is less in ClH:pyridine than in ClH:NH_3. In a sense this result is counter to expectation. The ClH:pyridine complex has more proton-shared character than the ClH:NH_3 complex and may be expected to show greater coupling between the dimer- and proton-stretching vibrations. The smaller observed coupling may be a reflection of the greater mass of pyridine.

The experimental IR spectrum of ClH:pyridine has been measured in Ar and N_2 matrices.[10] In an Ar matrix there are two strong bands that have been attributed to the complex. The stronger band appears at 838 cm^{-1}, while the weaker band is at 1050 cm^{-1}. In an N_2 matrix there are four bands with frequencies of 1135, 875, 759, and 595 cm^{-1}. The appearance of multiple bands in these spectra has been attributed to coupling between the proton-stretching vibration and local vibrational modes of the pyridine ring.[10] It is also possible that two of the bands in the spectrum obtained in N_2 may be the components of a Fermi doublet.[10] Coupling between the proton-stretching mode and local modes of the pyridine ring can occur because of the dramatic decrease in the frequency of the proton-stretching vibration in the complex, which places it in the same region of

TABLE 3: Harmonic, One-Dimensional (1-D), and Two-Dimensional (2-D) Dimer- and Proton-Stretching Frequencies (cm^{-1}) for ClH:Pyridine as a Function of Field Strength (au)

	harmonic		anharmonic			
field	dimer	proton	dimer (1-D)	dimer (2-D)	proton (1-D)	proton (2-D)
0.0000	140[a]	1954[a]	144	185	1365	1289
0.0010	156	1794	148	214	1117	1170
0.0020	154	1426	164	246	1008	1075
0.0040	311	871	308	291	1249	971
0.0055	274	1368	268	295	1204	1010
0.0100	209	2142	202	231	1513	1546
expt Ar[b,c] 838, 1050						
expt N_2[b,d] 1135, 875, 759, 595						

[a] The zero-field harmonic dimer- and proton-stretching frequencies obtained from the full surface are 128 and 1964 cm^{-1}, respectively. [b] Reference 10. [c] The 838 cm^{-1} band is the stronger of the two bands. [d] Two of these bands may be components of a Fermi doublet.

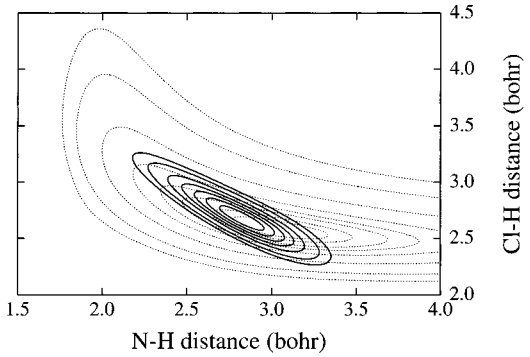

Figure 1. The square of the ground-state vibrational wave function superimposed on the zero-field potential surface. Contour values are at 0.0005, 0.001, 0.002, 0.003, 0.005, 0.01, 0.02, and 0.03 hartree above the global minimum. The same contour values appear in Figures 2 and 3.

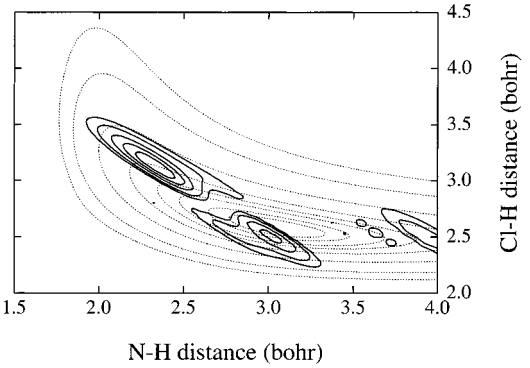

Figure 2. The square of the vibrational wave function for the $v = 1$ state of the proton-stretching mode superimposed on the zero-field potential surface. The proton-stretching wave function was calculated using a basis of 4900 dvr points to ensure convergence.

the spectrum as the pyridine ring vibrations. Coupling occurs between vibrations of the same symmetry (a_1) and similar energies.

The computed harmonic frequency of 1954 cm^{-1} is significantly greater than the experimental proton-stretching frequencies in both Ar and N_2. While the anharmonic two-dimensional frequency of 1289 cm^{-1} is in better agreement with experiment than the harmonic frequency, it is still too high relative to the experimental low-temperature matrix values. This difference may be attributed to at least two factors.

1. The computed two-dimensional anharmonic frequency refers to an isolated gas-phase complex. This computed frequency should be a reasonable estimate of the experimental gas-phase frequency if one could be measured. It is known that the matrix can have a dramatic effect on the spectra of hydrogen-bonded complexes with HCl and HBr.[1,10] In a subsequent section we will model the matrix effect by applying external electric fields.

2. The experimental spectra give evidence of coupling between the proton-stretching mode and local modes of the pyridine ring. Since the geometry of the pyridine ring is frozen in the two-dimensional anharmonic treatment of the potential surface, it is not possible for this treatment to account for such coupling. In future studies we intend to extend the anharmonic treatment to higher dimensions to include coupling between the proton-stretching vibration and modes other than the dimer stretch.

Figures 1 and 2 show plots of the square of the vibrational wave functions for the ground state and the $v = 1$ state of the proton-stretching vibration, respectively, superimposed on the zero-field potential surface. The ground state wave function is not centered directly over the minimum, but is displaced toward the proton-shared region of the surface, indicating that the system samples the proton-shared region even in the ground vibrational state. The wave function for the $v = 1$ state of the proton-stretching vibration is significantly displaced from the minimum toward the proton-shared region of the surface. In the $v = 1$ state, there is an even higher probability of finding the complex in this region. These features give rise to the large anharmonicity correction found for the proton-stretching vibration. In addition, there is mixing between the $v = 1$ state of the proton-stretching vibration and the $n = 8$ overtone of the dimer stretch, which have energies of 1289 and 1293 cm^{-1}, respectively, and are nearly accidentally degenerate. Such mixing was observed previously,[1] and gives rise to the "wobbles" in the plot shown in Figure 2.

The expectation values (R_0) of the Cl−N and Cl−H distances in the ground vibrational state are also reported in Table 2. The complex can access the proton-shared region of the surface even in the ground state and, since the Cl−N distance for a proton-shared hydrogen bond is shorter than the Cl−N distance for a traditional hydrogen bond, the expectation value [R_0 (Cl−N)] is shorter than [R_e(Cl−N)], in contrast to the usual relationship between R_e and R_o. At lower fields strengths [R_0 (Cl−H)] is greater than [R_e(Cl−H)]; however, [R_e(Cl−H)] is greater than [R_0(Cl−H)] at higher fields.

Structural and IR Results in the Presence of Electric Fields. As noted previously,[1] external electric fields preferentially stabilize more polar structures. Since the dipole moment increases as hydrogen-bond type changes from traditional, to proton-shared, to ion-pair, a smooth transition among these structures should be observed as a function of increasing field strength. Table 2 reports equilibrium distances and ground-state expectation values for Cl−N and Cl−H distances as a function

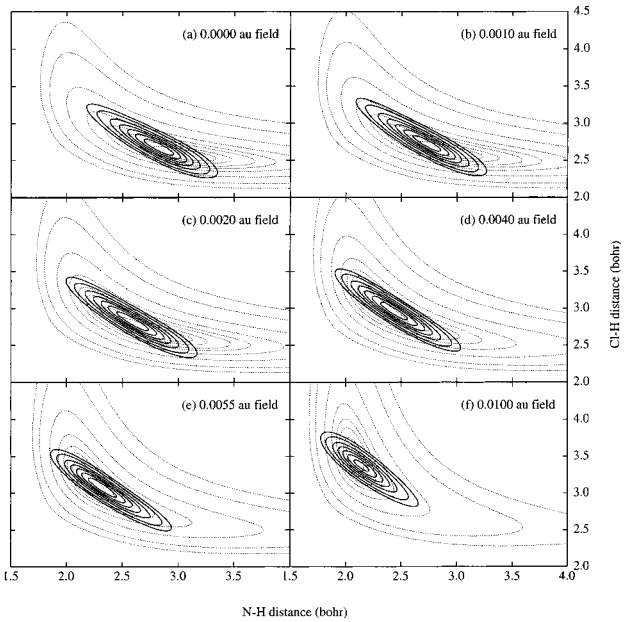

Figure 3. Plots of the square of the ground-state vibrational wave functions superimposed on the potential surfaces at varying field strengths.

of field strength. As the field strength increases, the Cl−N distance decreases to a minimum distance of 2.820 Å at a field of 0.0040 au. This suggests that the structure of the complex at this field strength is close to quasi-symmetric; that is, the forces on the proton from the Cl and the N are equal. The expectation value of the Cl−N distance is also a minimum at a field of 0.0040 au, although the change in R_0(Cl−N) as a function of field strength is not as dramatic as the change in R_e(Cl−N). Both R_0 and R_e values for Cl−H increase continuously as the field strength increases and the proton is transferred from Cl to N.

Figure 3 shows plots of the square of the ground-state vibrational wave functions superimposed on the potential surfaces at field strengths of 0.0000, 0.0010, 0.0020, 0.0040, 0.0055, and 0.0100 au. As a function of field strength, the minimum on the surface moves from the region associated with a traditional hydrogen bond, to the proton-shared region, and then to the region of the hydrogen-bonded ion pair. At a field strength of 0.0040 au, the minimum describes a very broad valley and the ground-state wave function describes a proton-shared hydrogen-bonded complex that is close to quasi-symmetric. As the field increases, the wave function describes complexes with increasing ion-pair character.

Changes in the Cl−N distance as a function of field strength are paralleled by changes in the computed anharmonic two-dimensional proton-stretching frequencies. As evident from Table 3, this frequency initially decreases as the field is turned on, exhibits its minimum value of 971 cm^{-1} at a field strength of 0.0040 au, and then increases to 1010 and 1546 cm^{-1} at fields of 0.0055 and 0.0100 au, respectively.

The gas-phase zero-field structure of ClH:pyridine has a larger dipole moment than $ClH:NH_3$ but a smaller dipole moment than $ClH:N(CH_3)_3$, as shown in Table 1. The ClH:pyridine complex, however, is significantly larger than either $ClH:NH_3$ or $ClH:N(CH_3)_3$ and the calculated Onsager reaction fields, at a given relative permittivity, are lower for ClH:pyridine than for the other two complexes. At field strengths of 0.0010 and 0.0020 au, the two-dimensional anharmonic proton-stretching frequencies of ClH:pyridine are 1170 and 1075 cm^{-1}, respectively. These values are higher than the stronger of the two bands in

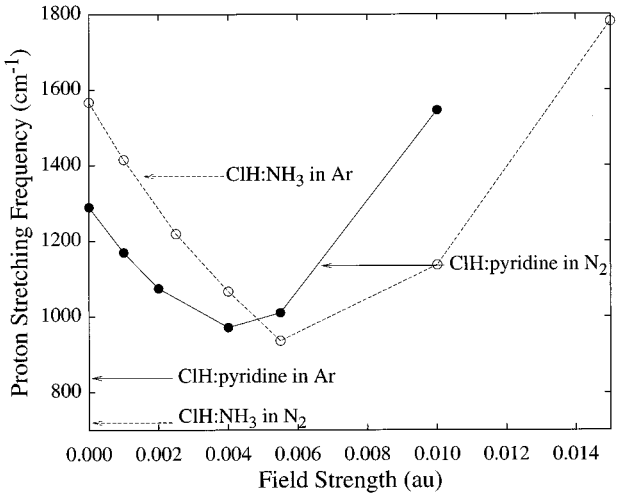

Figure 4. ClH:pyridine and $ClH:NH_3$ proton-stretching frequencies as a function of field strength. (—) ClH:pyridine. (- —) $ClH:NH_3$. Experimental frequencies in Ar and N_2 are as indicated.

the Ar matrix spectrum of this complex, which is found at 838 cm^{-1}.[10] The lowest calculated two-dimensional anharmonic proton stretching frequency is 971 cm^{-1} at a field strength of 0.0040 au. This value is still 133 cm^{-1} higher than experiment. There are three sources for the discrepancy between the two-dimensional proton-stretching frequency and the experimental value. The model we have used for the matrix environment employs an isotropic external field, and this is an oversimplification because the reaction field will change as the structure of the complex changes (eq 1). The second source of error is the dimensionality of the anharmonic calculations. We have already ascertained that coupling of the proton-stretching vibration to the pyridine ring modes is important,[10] and this coupling cannot be taken into account in a two-dimensional treatment. The third source of error arises from the fact that the ClH:pyridine potential energy surfaces have been calculated with pyridine frozen at its zero-field equilibrium geometry in the complex. Again this is an oversimplification since the pyridine geometry will relax as the proton moves, lowering the potential energy and leading to lower vibrational frequencies. Future work will address these factors. Nevertheless, the results of Tables 1 and 3 suggest that in Ar, the equilibrium ClH:pyridine complex has a hydrogen bond on the traditional side of quasi-symmetric.

In an N_2 matrix there are 4 bands arising from the ClH:pyridine complex, with frequencies of 1135, 875, 759, and 595 cm^{-1}.[10] Since an N_2 matrix has a stronger interaction with a complex than an Ar matrix, it is expected that ClH:pyridine in N_2 should lie on the ion-pair side of quasi-symmetric. This is consistent with the observation of a strong band at 1135 cm^{-1} in the experimental spectrum, and with the computed anharmonic proton-stretching frequencies of 1010 and 1546 cm^{-1} at field strengths of 0.0055 and 0.0100 au, respectively. The shift to higher frequency suggests that the proton-stretching band has increased N−H stretching character. This is also consistent with the increase in the Cl−N distance as the field strength increases above 0.0040 au. The conclusions about the nature of the hydrogen bond in ClH:pyridine in Ar and N_2 resulting from the two-dimensional treatment of ClH:pyridine presented in this work are in agreement with observations made in ref 10, which were based on a very different approach.

The two-dimensional proton-stretching frequencies for ClH:pyridine and $ClH:NH_3$ are plotted against field strength in Figure 4. The minimum frequency for the proton-stretching vibration in ClH:pyridine is found at a field of 0.0040 au, whereas the

TABLE 4: Cl−N Spin−Spin Coupling Constants [$^{2h}J(^{35}Cl-^{15}N)$, Hz] Across the Cl−H−N Hydrogen Bond in ClH:Pyridine and ClH:NH_3 as a Function of Field Strength (au)

field	ClH:pyridine implicit[a] FC[d]	ClH:NH_3 implicit[a,b] FC[d]	ClH:NH_3 implicit[a,b] $^{2h}J_{Cl-N}$	ClH:NH_3 explicit[c] FC[d]
0.0000	−9.3	−5.9	−5.7	−5.9
0.0010	−10.4	−6.3	−6.1	−6.6
0.0020	−12.1			
0.0025		−7.1	−6.9	−7.8
0.0040	−13.9	−8.2	−8.0	−9.3
0.0055	−12.6	−12.2	−11.8	−13.5
0.0100	−9.3	−9.5	−9.1	−10.9
0.0150		−7.0	−6.7	−8.2

[a] Computed using the optimized geometry (R_e) for each complex at the indicated field strength, but with the field turned off. [b] Data taken from ref 8. [c] Computed using the optimized geometry (R_e) for each complex at the indicated field strength, with the field turned on. [d] The Fermi-contact term.

minimum for ClH:NH_3 occurs at a field of 0.0055 au. The experimental frequencies for these two complexes in Ar and N_2 matrices are also indicated in Figure 4. It is apparent from Figure 4 that the quasi-symmetric hydrogen bond is formed at a lower field strength in the ClH:pyridine complex. This is consistent with the fact that the zero-field structure of ClH:pyridine has more proton-shared character than that of ClH:NH_3. It is also consistent with the suggestion that the hydrogen bond in the ClH:pyridine complex is on the traditional side of quasi-symmetric in Ar and on the ion-pair side of quasi-symmetric in N_2. By comparison, ClH:NH_3 has less proton-shared character in Ar, and is close to quasi-symmetric in N_2.

It is appropriate at this point to comment on the harmonic and one- and two-dimensional anharmonic proton-stretching frequencies as a function of field strength. The harmonic frequency is significantly higher than the two-dimensional anharmonic frequency at all field strengths except 0.0040 au, as evident in Table 3. At this field the computed harmonic frequency is actually lower than the two-dimensional anharmonic frequency, and in good agreement with the experimental frequency of the stronger band in an Ar matrix. However, the region surrounding the minimum on the 0.0040 au potential surface is very flat which implies that the harmonic approximation is inappropriate. Therefore, the agreement between the harmonic frequency and the strong band in the experimental Ar matrix spectrum must be regarded as fortuitous. The one-dimensional anharmonic proton-stretching frequencies do not exhibit a consistent pattern as a function of field strength, and can be either higher or lower than the corresponding two-dimensional frequency. The one-dimensional anharmonic frequency is lowest at a field of 0.0020 au, and is surprisingly large at a field of 0.0040 au. This apparent anomaly is related to the curvature of the 0.0040 au surface, and the inability of a one-dimensional anharmonic treatment of vibration to adequately describe the region surrounding the minimum along a single normal-coordinate vector.

NMR Properties. Table 4 reports $^{35}Cl-^{15}N$ spin−spin coupling constants ($^{2h}J_{Cl-N}$) for the equilibrium structures of ClH:pyridine at each field strength, and corresponding data for ClH:NH_3. The coupling constants for ClH:pyridine are reported as implicit functions of field strength; that is, the coupling constants have been computed for the optimized structure at each field, but with the field turned off. The coupling constants for ClH:NH_3 reported in Table 4 have been computed as both implicit and explicit functions of field strength. The implicit calculations are reproduced from ref 8. The explicit values, that is, the coupling constant calculated at the optimized structure at each field, in the presence of the field, are reported for the first time in this paper. Turning on the external field during the calculation increases the absolute value of the coupling constant, but the trend as a function of field strength remains the same. While the field polarizes the electron density toward the chlorine, it reduces the electron density on the hydrogen-bonded proton, and this leads to Cl−N coupling constants with larger magnitudes.

TABLE 5: NMR Chemical Shifts {$\delta[\delta(\text{ppm})]$} of the Hydrogen-Bonded Proton in ClH:Pyridine as a Function of Field Strength (au)

field	$\delta[\delta(\text{ppm})]$[a]
0.0000	13.2
0.0010	14.6
0.0020	16.9
0.0040	22.7
0.0055	22.7
0.0100	21.3

[a] Shifts are relative to HCl.

As evident from Table 4, the absolute value of the Cl−N coupling constant in ClH:pyridine increases as the strength of the external field increases, is a maximum at a field of 0.0040 au, and then decreases as the field increases to 0.0055 and 0.0100 au. This behavior follows the same pattern as the changes in the intermolecular Cl−N distance and in the anharmonic proton-stretching frequency of the hydrogen-bonded proton. This is not unexpected, given that both proton-stretching frequencies and coupling constants exhibit extremum values for complexes with quasi-symmetric hydrogen bonds, and these are associated with short intermolecular distances. Thus, the X−Y coupling constant across an X−H−Y hydrogen bond and the anharmonic two-dimensional proton-stretching frequency again appear to be fingerprints for hydrogen bond type.[8]

Table 5 reports ^1H NMR chemical shifts for the hydrogen-bonded proton for equilibrium ClH:pyridine structures as a function of field strength. The shifts reported are relative to the HCl monomer. The NMR chemical shift is 13.2 ppm in the zero-field structure, increases to 22.7 ppm in the equilibrium structures at field strengths of 0.0040 and 0.0055 au, and then decreases slightly in the ion-pair structure at a field of 0.0100 au. While the chemical shift of the hydrogen-bonded proton has its maximum value for the quasi-symmetric proton-shared structure, the variation of proton chemical shift with field strength is not as dramatic as the variation in coupling constants and proton-stretching frequencies. At the higher fields, that is, in the structures with ion-pair character, the proton chemical shift does not decrease with increasing Cl−N distance as rapidly as the absolute value of the coupling constant decreases and the proton-stretching frequency increases. This is also true for the proton chemical shift in ClH:NH_3.[8] Figure 5 shows a plot of the Cl−N distance, the anharmonic proton-stretching frequency, the magnitude of the Cl−N coupling constant, and the proton chemical shift of the hydrogen-bonded proton for ClH:pyridine as a function of field strength. This plot demonstrates graphically that the chemical shift of the hydrogen-bonded proton may not be as useful for structure determination as the coupling constant across the hydrogen bond and the proton-stretching frequency.

Limbach et al.[41] have reported an elegant NMR study of the temperature-dependent solvent electric field effects on proton transfer and hydrogen bond geometries in complexes of various acids with pyridine. They measured chemical shifts of the hydrogen-bonded proton, and scalar coupling constants ($^{1h}J_{H-N}$)

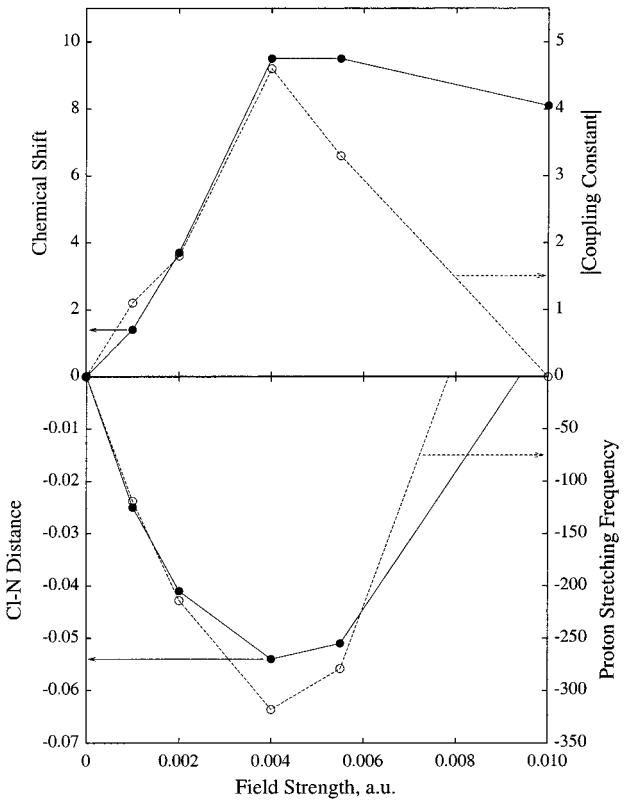

Figure 5. Structural, vibrational, and NMR properties of the ClH:pyridine complex as a function of the strength of an external field imposed along the Cl−H−N direction. These plots have been made relative to a value of 0.0 for the property at zero field. The absolute values of the properties are given in the tables. The upper plot shows the proton chemical shift (solid line) and the Cl−N spin−spin coupling constant (dashed line) as implicit functions of field strength. The lower plot shows the proton-stretching frequency (dashed line) and the equilibrium Cl−N distance (solid line) as explicit functions of field strength.

TABLE 6: Expectation Values of the Cl−N and Cl−D Distances [R_0(Cl−N), R_0(Cl−D), Å] in the Ground Vibrational State and Harmonic, One-Dimensional (1-D), and Two-Dimensional (2-D) Dimer- and Proton-Stretching Frequencies (cm^{-1}) as a Function of Field Strength (au) for ClD:Pyridine

					anharmonic			
			harmonic		dimer		proton	
field	R_0(Cl−N)	R_0(Cl−D)	dimer	proton	1-D	2-D	1-D	2-D
0.0000	2.927	1.421	138	1411	142	160	1139	979
0.0010	2.894	1.454	154	1297	146	183	912	860
0.0020	2.870	1.492	150	1040	161	220	690	757
0.0040	2.850	1.571	310	620	307	292	796	658
0.0055	2.856	1.628	273	977	266	294	784	715
0.0100	2.925	1.789	208	1527	201	220	1193	1200

for the hydrogen-bonded proton and the pyridine nitrogen. Their interpretations are consistent with the findings of this work. In particular, they noted that decreasing temperature leads to an increased electric field on hydrogen-bonded complexes, resulting in a change of hydrogen bond type from traditional, to proton-shared, to ion pair. At the quasi-symmetric structure the hydrogen bond distance is contracted, and for ClH:pyridine, the quasi-symmetric structure gives rise to the maximum value of the proton chemical shift.

ClD:Pyridine. Table 6 reports ground-state expectation values for Cl−N and Cl-D distances as a function of field strength for the ClD:pyridine complex together with harmonic and anharmonic stretching frequencies for the dimer- and proton-stretching modes. At the lower field strengths of 0.0000 and 0.0010 au, the expectation value of the Cl−N distance R_0(Cl−N) is slightly larger in ClD:pyridine than that in ClH:pyridine. At higher fields R_0(Cl−N) is smaller in the deuterated complex, except at the highest field strength of 0.0100 au. At field strengths of 0.0000, 0.0010, and 0.0020 au, the expectation value of the Cl-D distance, R_0(Cl-D), is smaller than the corresponding R_0(Cl−H). The combination of a larger R_0(Cl−N) and a smaller R_0(Cl−D) suggests that, at lower fields, the ClD:pyridine complex has less proton-shared character than the ClH:pyridine complex. When the complex is close to quasi-symmetric R_0(Cl−N) is notably smaller in the deuterated species. This is indicative of the fact that ClD:pyridine sits lower in the potential well, and does not sample the proton-shared region of the surface as extensively. The minima in both R_0(Cl−N) and the two-dimensional anharmonic proton-stretching frequency occur at a field strength of 0.0040 au for both ClD:pyridine and ClH:pyridine.

The proton-stretching frequency is reduced when DCl replaces HCl, as evident from Tables 3 and 6. Harmonic analysis gives a value of 0.71 for the ratio υ(D)/υ(H). The anharmonic ratio υ(D)/υ(H) for the one- or two-dimensional proton stretching frequencies is smallest when the hydrogen bond is proton-shared at field strengths of 0.0020, 0.0040, and 0.0055 au. In these cases both one- and two-dimensional ratios fall at or below the harmonic value of 0.71. At smaller or larger fields, when the hydrogen bonds have more traditional or ion-pair character, the ratio υ(D)/υ(H) is significantly larger than the harmonic prediction. These trends are similar to those observed previously for ClH:NH_3, BrH:NH_3, ClH:$N(CH_3)_3$ and BrH:$N(CH_3)_3$ and their deuterated analogues.[1,3] To our knowledge, the experimental IR spectrum of ClD:pyridine has not been recorded.

Conclusions

The following statements about the hydrogen-bonded ClH:pyridine complex are supported by the calculations carried out in this study.

1. The zero-field equilibrium structure of ClH:pyridine is stabilized by a traditional Cl−H···N hydrogen bond, although the degree of proton transfer from Cl to N is greater in this complex that in the ClH:NH_3 complex.

2. The computed gas-phase anharmonic proton-stretching frequency of ClH:pyridine is 1289 cm^{-1}. This frequency initially decreases as the strength of the external field increases, and exhibits a minimum value of 971 cm^{-1} for a complex which has a proton-shared hydrogen bond that is close to quasi-symmetric at a field strength of 0.0040 au. The proton-stretching frequency subsequently increases with increasing field as the stretching vibration becomes a perturbed N−H stretch in complexes that have greater ion-pair character.

3. The experimental IR spectrum of ClH:pyridine in Ar has a strong proton-stretching band at 838 cm^{-1} and a weaker band at 1050 cm^{-1}. In an N_2 matrix 4 bands are observed at 1135, 875, 759, and 595 cm^{-1}. Our calculations suggest that the ClH:pyridine complex is on the traditional side of quasi-symmetric in Ar and on the ion-pair side of quasi-symmetric in N_2.

4. As a function of field strength, the intermolecular Cl−N distance and the anharmonic proton-stretching frequency initially decrease, exhibit minimum values for the quasi-symmetric hydrogen-bonded complex at a field of 0.0040 au, and then subsequently increase as the strength of the external field increases. The magnitude of the Cl−N coupling constant across the hydrogen bond initially increases as the field strength increases, exhibits a maximum at a field of 0.0040 au, and then

decreases with increasing field strength. Thus, the structure of a hydrogen-bonded complex in terms of the intermolecular distance can be determined from the spectroscopic properties of proton-stretching frequency and spin−spin coupling constant across the hydrogen bond. Although the chemical shift of the hydrogen-bonded proton also has its maximum value at a field of 0.0040 au, it does not decrease dramatically at higher fields, and may not be as useful an indicator of hydrogen bond type and intermolecular distance.

5. Deuteration of HCl lowers the anharmonic proton-stretching frequencies in ClD:pyridine at all field strengths considered, although the ratio υ(D)/υ(H) may be higher or lower than the harmonic value of 0.71. The trends in the expectation values of the Cl−N distance and the anharmonic proton-stretching frequencies are the same in ClD:pyridine and ClH:pyridine.

Acknowledgment. This work was supported by a grant from the National Science Foundation (CHE-9873815) and from the Australian Research Council (A2543). The authors are grateful to NSF, ARC, and the Ohio Supercomputer Center for support of this work. The authors also acknowledge many enlightening discussions with Drs. Willis Persons and Krystyna Szczepaniak on the experimental spectra of ClH-4-R-pyridine complexes.

References and Notes

(1) Jordan, M. J. T.; Del Bene, J. E. *J. Am. Chem. Soc*. **2000**, *122*, 2101.
(2) Onsager, L. *J. Am. Chem. Soc*. **1936**, *58*, 1486.
(3) Bevitt, J.; Chapman, K.; Crittenden, D.; Jordan, M. J. T.; Del Bene, J. E. *J. Phys. Chem. A* **2001**, *105*, 3371.
(4) Ramos, M.; Alkorta, I.; Elguero, J.; Golubev, N. S.; Denisov, G. S.; Benedict, H.; Limbach, H.-H. *J. Phys. Chem. A* **1997**, *101*, 9791.
(5) Yin, J.; Green, M. E. *J. Phys. Chem. A* **1998**, *102*, 7181.
(6) Benedict, H.; Limbach, H.-H.; Wehlan, M.; Fehlhammer, W.-P.; Golubev, N. S.; Janoschek, R. *J. Am. Chem. Soc*. **1998**, *120*, 2939.
(7) Benedict, H.; Shenderovich, I. G.; Malkina, O. L.; Malkin, V. G.; Denisov, G. S.; Golubev, N. S.; Limbach, H.-H. *J. Am. Chem. Soc*. **2000**, *122*, 1979.
(8) Del Bene, J. E.; Jordan, M. J. T. *J. Am. Chem. Soc*. **2000**, *122*, 4794.
(9) Del Bene, J. E.; Jordan, M. J. T. *J. Chem. Phys*. **1998**, *108*, 3205.
(10) Szczepaniak, K.; Chabrier, P.; Person, W. B.; Del Bene, J. E. *J. Mol. Struct*. **2000**, *520*, 1.
(11) Legon, A. C. *Chem. Soc. Rev*. **1993**, *22*, 153.
(12) Cooke, S. A.; Corlett, G. K.; Lister, D. G.; Legon, A. C. *J. Chem. Soc., Faraday Trans*. **1998**, *94*, 837.
(13) Barnes, A. J.; Wright, M. P. J. *J. Chem. Soc., Faraday Trans. 2* **1986**, *82*, 153.
(14) Barnes, A. J.; Beech, T. R.; Mielke, Z. *Chem. Soc., Faraday Trans. 2* **1984**, *80*, 455.
(15) Pople, J. A.; Binkley, J. S.; Seeger, R. *Int. J. Quantum Chem. Quantum Chem. Symp*. **1976**, *10*, 1.
(16) Krishnan, R.; Pople, J. A. *Int. J. Quantum Chem*. **1978**, *14*, 91.
(17) Bartlett, R. J.; Silver, D. M. *J. Chem. Phys*. **1975**, *62*, 3258.
(18) Bartlett, R. J.; Purvis, G. D. *Int. J. Quantum Chem*. **1978**, *14*, 561.
(19) Dunning, T. H., Jr. *J. Chem. Phys*. **1989**, *90*, 1007.
(20) Kendall, R. A.; Dunning, T. H., Jr.; Harrison, R. J. *J. Chem. Phys*. **1992**, *96*, 1358.
(21) Woon, D. E.; Dunning, T. H., Jr. *J. Chem. Phys*. **1993**, *98*, 1358.
(22) Del Bene, J. E. In *Encyclopedia of Computational Quantum Chemistry*; Schleyer, P. v. R., Allinger, N. L., Clark, T., Gasteiger, J., Kollman, P. A., Schaefer, H. F., III., Schreiner, P. R., Eds.; Wiley: Chichester, UK, 1998; Vol. 2.
(23) Del Bene, J. E.; Shavitt, I. In *Molecular Interactions: From van der Waals to Strongly Bound Complexes*; Scheiner, S., Ed.; John Wiley and Sons: Sussex, 1997; pp 157−179.
(24) Del Bene, J. E.; Person, W. B.; Szczepaniak, K. *J. Phys. Chem*. **1995**, *99*, 10705.
(25) Del Bene, J. E.; Jordan, M. J. T. *Int. Rev. Phys. Chem.* **1999**, *18*, 119.
(26) Bacic, Z.; Light, J. C. *Annu. Rev. Phys. Chem*. **1989**, *40*, 469.
(27) Wei, H.; Carrington, T., Jr. *J. Chem. Phys*. **1992**, *97*, 3029.
(28) Perera, S. A.; Sekino, H.; Bartlett, R. J. *J. Chem. Phys*. **1994**, *101*, 2186.
(29) Perera, S. A.; Nooijen, M.; Bartlett, R. J. *J. Chem. Phys*. **1996**, *104*, 3290.
(30) Perera, S. A.; Bartlett, R. J. *J. Am. Chem. Soc*. **1995**, *117*, 8476.
(31) Perera, S. A.; Bartlett, R. J. *J. Am. Chem. Soc*. **1996**, *118*, 7849.
(32) Del Bene, J. E.; Perera, S. A.; Bartlett, R. J. *J. Am. Chem. Soc*. **2000**, *122*, 3560.
(33) Schafer, A.; Horn, H.; Alhrichs, R. *J. Chem. Phys*. **1992**, *97*, 2571.
(34) Perera, S. A.; Bartlett, R. J. *J. Am. Chem. Soc*. **2000**, *122*, 1231.
(35) Del Bene, J. E.; Perera, S. A.; Bartlett, R. J.; Alkorta, I.; Elguero, J. *J. Phys. Chem. A.* **2000**, *104*, 7165.
(36) Del Bene, J. E.; Bartlett, R. J. *J. Am. Chem. Soc*. **2000**, *122*, 10480.
(37) Gauss, J. *Chem. Phys. Lett*. **1992**, *191*, 614.
(38) Frisch, M. J.; Trucks, G. W.; Schlegel, H. B.; Scuseria, G. E.; Robb, M. A.; Cheeseman, J. R.; Zakrzewski, V. G.; Montgomery, J. A., Jr.; Stratmann, R. E.; Burant, J. C.; Dapprich, S.; Millam, J. M.; Daniels, A. D.; Kudin, K. N.; Strain, M. C.; Farkas, O.; Tomasi, J.; Barone, V.; Cossi, M.; Cammi, R.; Mennucci, B.; Pomelli, C.; Adamo, C.; Clifford, S.; Ochterski, J.; Petersson, G. A.; Ayala, P. Y.; Cui, J.; Morokuma, K.; Malick, D. K.; Rabuck, A. D.; Raghavachari, K.; Foresman, J. B.; Cioslowski, J.; Ortiz, J. V.; Baboul, A. G.; Stefanov, B. B.; Liu, G.; Liashenko, A.; Piskorz, P.; Komaromi, I.; Gomperts, R.; Martin, R. L.; Fox, D. J.; Keith, T.; Al-Laham, M. A.; Peng, C. Y.; Nanayakkara, A.; Gonzalez, C.; Challacombe, M.; Gill, P. M. W.; Johnson, B.; Chen, W.; Wong, M. W.; Andres, J. L.; Gonzalez, C.; Head-Gordon, M.; Replogle, E. S.; Pople, J. A. *Gaussian 98*; Gaussian, Inc.: Pittsburgh, PA, 1998.
(39) Marcoux, J. J. *J. Opt. Soc. Am.* **1969**, *59*, 998.
(40) ACES II is a program product of the Quantum Theory Project, University of Florida. Authors: Stanton, J. F.; Gauss, J.; Watts, J. D.; Nooijen, M.; Oliphant, N.; Perera, S. A.; Szalay, P. G.; Lauderdale, W. J.; Gwaltney, S. R.; Beck, S.; Balkova, A.; Bernholdt, D. E.; Baeck, K.-K.; Tozyczko, P.; Sekino, H.; Huber, C.; Bartlett, R. J. Ingetral packages included are VMOL (Almlof, J.; Taylor, P. R.); VPROPS (Taylor, P. R.); ABACUS (Helgaker, T.; Jensen, H. J. Aa.; Jorgensen, P.; Olsen, J.; Taylor, P. R.).
(41) Golubev, N. S.; Denisov, G. S.; Smirnov, S. N.; Shchepkin, D. N.; Limbach, H.-H. *Z. Phys. Chem.* **1996**, *196*, 73.